Chinese Journal of Chemistry, **2005**, *23*, 149—154 **Full Paper**

Molecule-Based Cobalt Hexacyanoferrate Nanoparticle: Synthesis, Characterization, and Its Electrochemical Properties

SHI, Li-Hong[a](史立红) WU, Tian[a](吴田) WANG, Mei-Jia[a](王美佳) LI, Di[a](李迪)
ZHANG, Yuan-Jian[a](张袁健) LI, Jing-Hong*[,a,b](李景虹)

[a] *State Key Laboratory of Electroanalytical Chemistry, Changchun Institute of Applied Chemistry, Chinese Academy of Sciences, Changchun, Jilin 130022, China*
[b] *Department of Chemistry, Tsinghua University, Beijing 100084, China*

Cobalt hexacyanoferrate (CoHCF) nanoparticles, with an average size of less than 50 nm for individual crystallite, were synthesized by simply mixing appropriate reactants in the absence of surfactant or template. Elemental analysis provided a stoichiometric formula, $K_{0.2}Co_{1.4}[Fe(CN)_6]\bullet xH_2O$ for this compound. The involvement of both ferromagnetic $Co^{II}_{1.5}[Fe^{III}(CN)_6]$ and antiferromagnetic $KCo^{III}[Fe^{II}(CN)_6]$ species in the CoHCF complex was effectively proved by Fourier transform infrared spectroscopy, so was the existence of certain amounts of interstitial water molecules. A glassy carbon electrode modified with these CoHCF nanoparticles had high stable and reversible cyclic voltammetric responses even at high scan rates and its electrochemical properties were affected by the nature of counter cations and the concentration of supporting electrolyte. The prepared nanoparticle films, as a mediator on electrode surface, exhibited considerable electrocatalytic activity toward the oxidation of dopamine.

Keywords nanoparticle, cobalt hexacyanoferrate, electrochemistry, electrocatalysis, dopamine

Introduction

Prussian blue (PB) and related metal hexacyanoferrate salts constitute a class of zeolitic mixed-valence compounds that have been investigated intensively due to their interesting properties, such as electrocatalysis,[1-6] electrochromism,[7-9] ion-exchange properties,[10,11] and charge storage capabilities.[12-14] Recently, PB analogues have played an important role in the field of molecular magnets for their high Curie temperature values, photomagnetic properties, and their structural aspects related to magnetic properties.[15-18] The synthesis and properties of these materials are of significant interest to a wide range of research areas, following which some nanoscale magnetic particles of PB analogues have been prepared as a series of new optical, electronic and magnetic materials.[19-22]

In spite of many unique characteristics of nanosized PB analogues, the electrochemistry of these materials, being of great significance for both fundamental research and practical application, was reported rarely.[23] Thus we chose an outstanding member of PB analogues, cobalt hexacyanoferrate (CoHCF) as a model system in the present work. It is known that CoHCF films are easier to be prepared and characterized by electrochemical method.[24-28] The existence of Co(II), Co(III), Fe(II), and Fe(III) redox centers results in a series of CoHCF compounds with various stoichiometries, which have been described in detail by Lezna *et al*. using a combination analysis of voltammetry, *in situ* infrared spectroelectrochemistry, and X-ray photoelectron spectroscopy.[29] In addition, CoHCF shows reversible photoinduced magnetization,[15,16] and unique electrochromic properties with color changes depend not only on the oxidation states of the Co/Fe ions but also on the nature of counter cations incorporated in it during electroreduction.[30,31] There are other reports on the electrocatalytic properties of CoHCF films for a variety of substrates, including ascorbic acid, hydroxylamine, glutathione, morphine, epinephrine, norephinephrine,[26,27,32-35] which can be employed for developing amperometric electrodes.

In this paper, CoHCF nanoparticles were synthesized without using surfactant or template, and characterized with several techniques such as UV/Vis spectroscopy, X-ray diffraction (XRD), electron diffraction (ED), and Fourier transform infrared (FT-IR) spectroscopy. Furthermore, the CoHCF nanoparticle films were electrodeposited on a glassy carbon electrode by cyclic voltammetry (CV) for investigating its electrochemical behavior and electrocatalytic properties toward dopamine oxidation.

Experimental

Chemicals

Dopamine was purchased from Sigma (USA) and used as received. All other chemicals were of analytical

* E-mail: jhli@mail.tsinghua.edu.cn; Tel. and Fax: (+86-010-62776949)
Received May 24, 2004; revised and accepted October 21, 2004.
Project supported by the National Natural Science Foundation of China (Nos. 20125513, 20435010).

grade and used without further purification. Dopamine solutions were prepared freshly with doubly distilled water. Water was purified with a Milli-Q (18.3 MΩ) water system.

Synthesis of CoHCF nanoparticles

The molecule-based CoHCF compound was prepared by the following procedures: 25 mL of $CoCl_2$ solution (20 mmol•L^{-1}) was slowly added to a vigorously stirred $K_3Fe(CN)_6$ solution (25 mL, 10 mmol•L^{-1}) in a beaker. After the addition, the mixture was stirred well for 3 h, then the precipitates were centrifuged twice and washed each time with 10 mL doubly distilled water to remove the excessive potassium ions and chloride ions. At last, the crude product was dried in an oven at 60 ℃ overnight.

Preparation of CoHCF films

A bare glassy carbon (GC) electrode was continuously scanned from 0.0 to 1.0 V in 0.1 mol•L^{-1} KCl solution containing 10 mmol•L^{-1} CoHCF (dispersed with ultrasonic wave) at a scan rate of 10 mV•s^{-1}. After 20 cycles the modified electrode was taken out, rinsed with doubly distilled water for several times, and stored in 0.1 mol•L^{-1} KCl solution before use. As described above, the nanoparticles have been formed before their deposition onto GC electrode, thus the films prepared here were different from that obtained by conventional methods.

Instruments

The UV/Vis spectrum of the diluted aqueous solution of CoHCF nanoparticles was recorded with a Cary-500 UV-Vis-NIR spectrophotometer (VARIAN, USA). XRD was performed on a RIGAKU D/max-IIB X-ray Diffractometer using Cu Kα radiation (0.15406 nm) of 40 kV and 20 mA at room temperature. A scan rate of 4° per minute was applied to record from a 2θ of 10° to 60°. Sample was mulled and placed on the glass holder providing for the instrument. ED was conducted on JEOL-JEM-2010 electron microscopy operating at 200 kV (JEOL, Japan). Sample for ED measurement was prepared by casting one drop of ethanol solution of CoHCF (being dispersed in ethanol with ultrasonic wave) onto a standard carbon-coated (20—30 nm) formvar film on copper grid (230 mesh). FT-IR spectroscopy was obtained with a FTS135 infrared spectroscope (BIO-RAD, USA). Transmission spectrum was obtained by forming a thin transparent KBr pellet containing the materials of interest. Inductive coupled plasma-atomic emission spectroscopy (ICP-AES) was conducted on a model POEMS spectrometer (Thermo Jarrell Ash Corporation, USA). The electrochemistry was preformed using a CHI Instrument model 832 (CHI Inc., USA) at room temperature. CV was carried out in a conventional three-electrode cell. An Ag/AgCl (saturated KCl) electrode, a platinum wire (99%, Aldrich) and a GC electrode (2.4 mm in diameter) were used as the reference, auxiliary and working electrodes, respectively. Prior to the experiment, the GC electrode was carefully polished with 1, 0.3 and 0.05 μm alumina polishing compounds respectively, ultrasonically cleaned in distilled water and blown dry with high-purity nitrogen. All solutions were bubbled with high purity nitrogen for about 20 min before each electrochemical experiment, and kept under a nitrogen atmosphere during the experiments.

Results and discussion

Characterization of the CoHCF nanoparticles

The UV/Vis absorption spectrum of the present compound is shown in Figure 1. As can be seen clearly, CoHCF exhibits an absorption maximum at about 390 nm, and a broad charge-transfer band between 500 and 600 nm attributed to the existence of mix-valence Fe-CN-Co sequence. This spectrum is identical with that of CoHCF precipitates dispersed and attached to glass slide.[28]

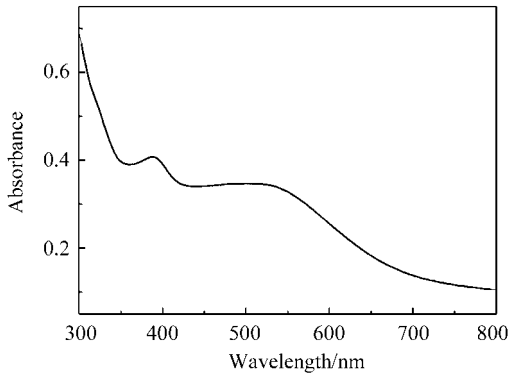

Figure 1 UV/Vis spectrum of CoHCF in aqueous phase.

Similar to PB, most metal hexacyanoferrates have a face-centered cubic structure, which has been suggested by Buser and co-workers.[36] The sharp, well-defined peaks shown in Figure 2 indicate that the compound is crystalline. The powder XRD pattern of CoHCF is with the reported face-centered cubic structure having a unit cell parameter of 1.03 nm. It exhibits four major diffraction peaks at 2θ values of 17.2°, 24.5°, 34.8°, and 39.1°, corresponding to the {200}, {220}, {400} and {420} reflections, respectively. The average crystallite size of CoHCF nanoparticles can be estimated by the Sherrer formula,[37]

$$D_{hkl}=0.9\lambda/(\beta_{hkl}\cos\theta) \quad (1)$$

where D_{hkl} is the crystallite size, λ the wavelength of the X-rays (0.15406 nm for Cu) in the present experiment, θ the diffraction angle, and β_{hkl} the full width at half maximum of the diffraction peak. The individual size of crystallite was calculated as 34.7 nm where {200} plane peak was used with $2\theta=17.2°$, indicating that the CoHCF synthesized here is nanosized complex. The samples were further characterized by TEM, from which their average diameter of ~50 nm was obtained.

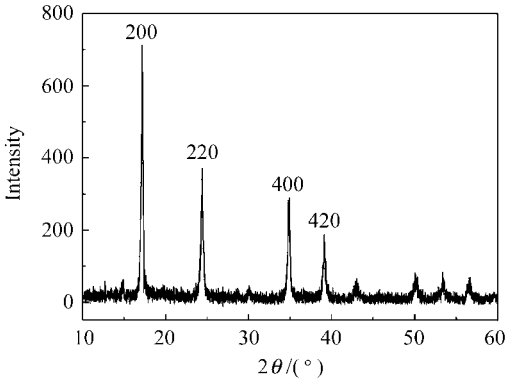

Figure 2 XRD pattern of CoHCF nanoparticles.

Figure 3 shows the ED pattern of the CoHCF nanoparticles in which there are several diffraction circles. The ED pattern revealed *d* spacings (0.52 nm of {200}; 0.36 nm of {220}; 0.26 nm of {400}; 0.23 nm of {420}) of face-centered cubic CoHCF structure.[21] Moreover, the results of ED analysis are comparable with that obtained above by the powder XRD analysis, which confirm further that the compound is a polycrystalline form of CoHCF.

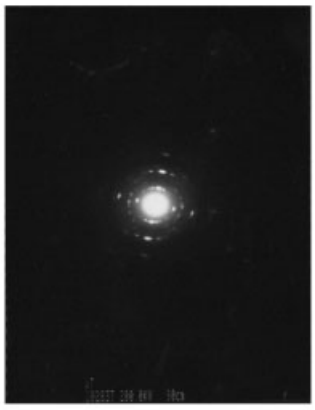

Figure 3 ED pattern of CoHCF nanoparticles.

Figure 4 shows the FT-IR spectroscopy of CoHCF nanoparticles in the region of 450 to 4000 cm^{-1}. The peaks at around 2159 and 2117 cm^{-1} can be assigned to the stretching of the CN group in the Fe^{III}-CN-Co^{II} and Fe^{II}-CN-Co^{III} environments, respectively.[29] Taking into account the stoichiometric formula $K_{0.2}Co_{1.4}[Fe(CN)_6]$ of the compound obtained by ICP-AES, one can conclude that both ferromagnetic $Co^{II}_{1.5}[Fe^{III}(CN)_6]$ and antiferromagnetic $KCo^{III}[Fe^{II}(CN)_6]$ species are implicated in the CoHCF complex. Absorption peaks at 592 and 541 cm^{-1} are attributed to the formation of Fe—C≡N—Co structure.[38] The bands at 3642 and 3401 cm^{-1} correspond to the stretching vibrations of the liberating and the associating O—H in CoHCF•xH_2O complex. Sato and co-workers[15] obtained an *x* value of 6.9 with the same Co/Fe ratio of 1.4 for the magnetic compound. The peak at 1610 cm^{-1} is ascribed to the bending vibration of H—O—H, which firmly provides evidence for the existence of crystal water in the structure of CoHCF.

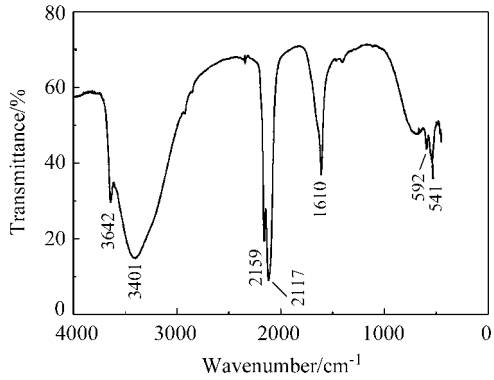

Figure 4 FT-IR spectrum of CoHCF nanoparticles. Several characteristic peaks are labeled.

Electrochemical characteristics of CoHCF nanoparticles

Figure 5 shows the repeated CVs of nanosized CoHCF deposition in 0.1 mol•L^{-1} KCl electrolyte solution. The films were found to have grown in thickness with the scan number, as exhibited by the increasing currents of both anodic and cathodic peaks. Also it was observed that all these peaks were not affected by stirring of the electrolyte, supplying proof for the irreversibility immobilization of CoHCF nanoparticles on the GC electrode.

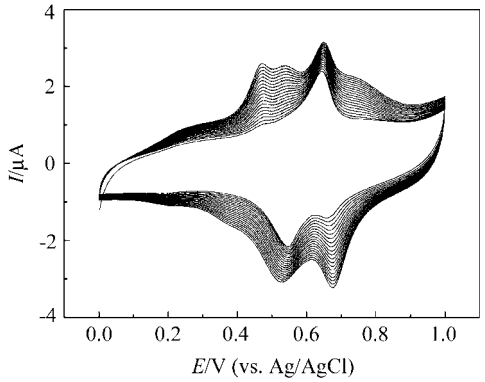

Figure 5 Consecutive cyclic voltammograms of a GC electrode modified with nanosized CoHCF prepared in 0.1 mol•L^{-1} KCl solution. Scan rate, 10 mV•s^{-1}.

The representative CVs obtained for CoHCF films in 0.1 mol•L^{-1} KCl solution at different scan rates are shown in Figure 6. Two sets of well-defined redox peaks can be observed clearly with formal potentials of 500 and 667 mV at a scan rate of 20 mV•s^{-1}. According to the experimental results of a combined use of CV and *in situ* IR spectroelectrochemistry obtained by Lezna *et al.*,[29] all the redox species of CoHCF were involved in the electrode reaction. As a result, the redox couple I at a lower potential was assigned to Co(III)/Co(II) transition and the redox couple II at a higher potential to Fe(III)/Fe(II) transition. The overall electrochemical processes of CoHCF films can be described by the fol-

lowing equations:

$$K_2Co^{II}[Fe^{II}(CN)_6]=KCo^{III}[Fe^{II}(CN)_6]+K^++e^- \quad (1)$$

$$K\,Co^{II}_{1.5}[Fe^{II}(CN)_6]=Co^{II}_{1.5}[Fe^{III}(CN)_6]+K^++e^- \quad (2)$$

As shown in Figure 6, the anodic peaks shift positively and the cathodic peaks shift negatively with increasing scan rate, leading to the change of potential separation between anodic and cathodic peaks (ΔE_p). For example, the ΔE_p value of redox couple II was about 5 mV at a low scan rate of 20 mV•s^{-1}, while it increased to more than 80 mV as the scan rate climbing to 100 mV•s^{-1}. Also the anodic peak currents (I_{pa}) of the voltammograms are proportional to the scan rates below 100 mV•s^{-1} (inset of Figure 6A), indicating the surface-controlled redox processes. In addition, it was found that reduction of the scan rate down to 10 mV•s^{-1} could induce splitting of the anodic peak I into two components (Figure 5), and the division of both anodic peaks was observed at 5 mV•s^{-1} in Figure 6B.

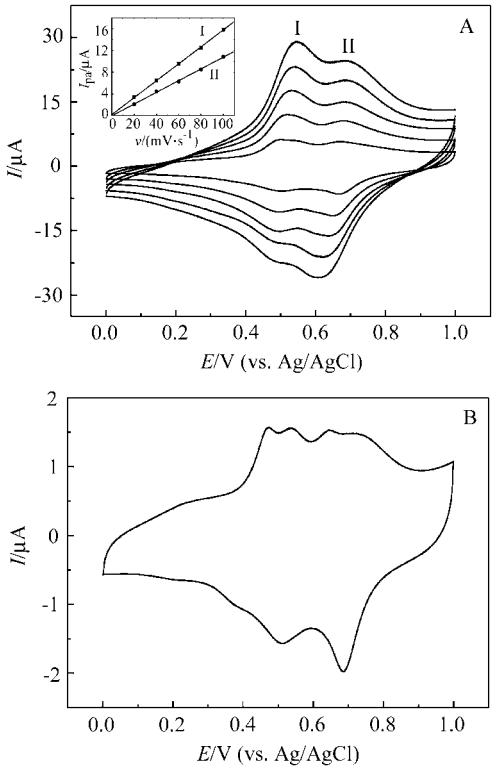

Figure 6 Cyclic voltammograms of nanosized CoHCF modified electrode in 0.1 mol•L^{-1} KCl solution at various scan rates. Scan rate (mV•s^{-1}), 20, 40, 60, 80 and 100 in Figure 6A, and 5 in Figure 6B. Inset (A) represents the plots of I_{pa} vs. scan rates for the redox couples I and II.

Ions usually enter or leave the complex in order to maintain the electroneutrality of the films during the experiments, for which they are bound to have a considerable effect on the electrochemical behaviors of the modified electrode. Figure 7 presents the effect of alkali metal cations and NH_4^+ on the electrochemical responses of CoHCF films. In K^+-containing solution, CoHCF films showed two pairs of well-defined redox peaks with formal potentials of about 510 and 660 mV as described previously (curve a). The cyclic voltammeric responses of the modified electrode in 0.1 mol•L^{-1} NaCl (curve b) or 0.1 mol•L^{-1} LiCl (curve c) were somewhat different in terms of formal potentials and the shape of peaks when compared to those obtained in 0.1 mol•L^{-1} KCl. Similar to the case in KCl, CoHCF films also exhibited two sets of redox peaks in Na^+ or Li^+-containing solution with one in negative and the other in positive direction shift. For example, the formal potentials of redox couple I in 0.1 mol•L^{-1} NaCl solution was 408 mV, and turned to a more negative value by 200 mV in 0.1 mol•L^{-1} LiCl. These results show that the formal potentials increased with increasing ionic radii of the cation.[39] In addition, the peak currents decreased obviously, accompanied by a little increase of ΔE_p, when Na^+ or Li^+-containing electrolyte solution was used instead of KCl solution, suggesting the less reversibility of the voltammetric behaviors of CoHCF films in these electrolyte solutions. The electrochemical responses of CoHCF films observed in NaCl and LiCl in our present case are not absolutely parallel with those reported before,[25-27] in all probability because of the different preparation methods and thicknesses of the CoHCF films used here and previously. In 0.1 mol•L^{-1} NH_4Cl medium, the voltammetric curve did not show obvious redox peak, indicating the loss of surface electrochemical activity of CoHCF films. The reason for this may be either the considerable difficulty of inserting NH_4^+ into CoHCF complex or the solubility of CoHCF in the supporting electrolyte.

In addition to the effect of the nature of cation, concentration of the electrolyte solution also can influence the electrode response of CoHCF films. The CVs in Figure 8 obviously show difference in peak potentials when the modified electrode was scanned in various

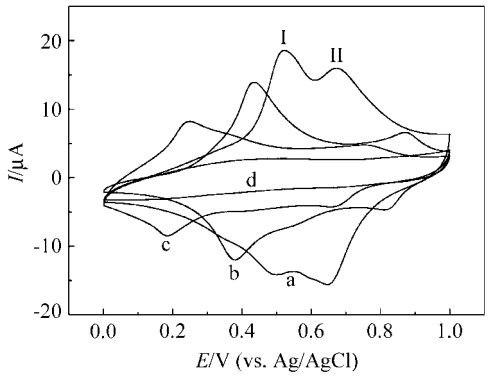

Figure 7 Cyclic voltammograms of nanosized CoHCF modified electrode in 0.1 mol•L^{-1} KCl (a), NaCl (b), LiCl (c) and NH_4Cl (d) supporting electrolyte solution at a scan rate of 40 mV•s^{-1}.

concentrations of KCl electrolyte. An increase of concentration by one decade led to the shift of formal potential of redox couple I by 52 mV in the positive direction, and the shift value was 56 mV for redox couple II, as well as the decrease of the redox couple current.

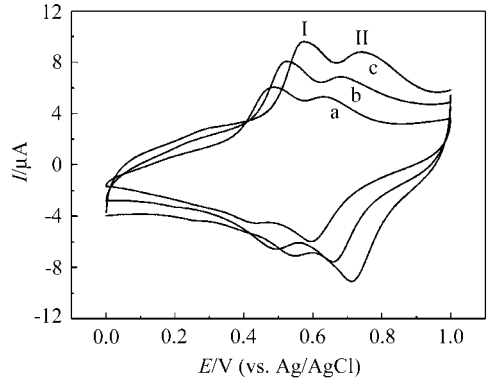

Figure 8 Cyclic voltammograms of nanosized CoHCF modified electrode in various concentration of KCl solution. (a) 0.01 mol•L^{-1}, (b) 0.1 mol•L^{-1} and (c) 1.0 mol•L^{-1}. Scan rate, 40 mV•s^{-1}.

The stability of the CoHCF films immobilized on the electrode surface was investigated by CV. Successive scanning of the modified electrode in 0.1 mol•L^{-1} KCl solution between 0.0 and 1.0 V for 3 h showed less than 10% decrease in the peak current, thus confirming its high stability for continuous use. Also the modified electrode can be stored in 0.1 mol•L^{-1} KCl at room temperature for at least one month, while showing no obvious change in the voltammetric response.

Electrocatalytic properties of CoHCF nanoparticles

In order to test the electrocatalytic behavior of CoHCF nanoparticles, CVs of the bare and CoHCF-coated GC electrode were scanned in 0.1 mol•L^{-1} KCl containing various concentrations of dopamine at 40 mV•s^{-1} (Figure 9). Dopamine is an important neurotransmitter in the mammalian central nervous system, and its electrochemistry is significant for research into electroanalytical chemistry and neurochemistry. However, the electrochemical response of dopamine is irreversible with a large peak-peak separation and high overpotential. The electrochemical reaction of dopamine at a bare GC electrode showed one redox couple with an anodic peak potential at 489 mV and a cathodic peak potential at 153 mV (curve a), the ΔE_p of which was of 336 mV. When CoHCF films was used for oxidation of dopamine with various concentrations (curves c—g), the oxidation potentials of dopamine shifted to negative direction while the reduction potentials to positive one, as a result of which the ΔE_p decreased to less than 160 mV. These experimental results show that the modification of GC electrode yielded a lower overpotential and a smaller peak-to-peak separation. Furthermore, both the anodic and cathodic peak currents increased with dopamine concentration. The inset of Figure 9 shows the plot of anodic peak current I_{pa} versus dopamine concentration between 0.0 and 2.8 mmol•L^{-1} with a correlation coefficient better than 0.999, which indicates that the electrocatalytic activity of CoHCF films towards dopamine oxidation can be considered for application in analytical purposes.

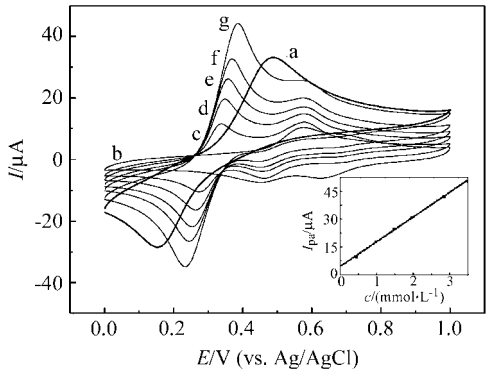

Figure 9 Cyclic voltammograms of the GC electrode in potassium hydrogen phthalate buffer solution (pH 5.0) containing 0.1 mol•L^{-1} KCl with different concentrations of dopamine. Bare GC electrode with 2.85 mmol•L^{-1} dopamine (a), and CoHCF modified GC electrode with dopamine concentration (mmol•L^{-1}): (b) 0.0, (c) 0.44, (d) 0.98, (e) 1.48, (f) 1.96 and (g) 2.85. Scan rate, 40 mV•s^{-1}. Inset represents the variations of I_{pa} vs. dopamine concentration.

Figure 10 shows the CVs of CoHCF films at various scan rates obtained in 0.1 mol•L^{-1} KCl containing 2.8 mmol•L^{-1} dopamine solution. It can be seen from Figure 10 that the anodic peak potential shifted slightly to the positive value and the cathodic peak potential shifted to the negative value with increasing scan rate, suggesting a kinetic limitation in the reaction between the redox sites of the CoHCF films and dopamine. In addition, both the anodic and cathodic currents gradually increased with the increase of scan rate. A linear

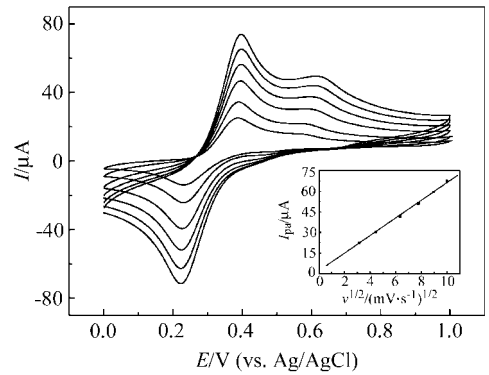

Figure 10 Cyclic voltammograms of 2.85 mmol•L^{-1} dopamine oxidation on a CoHCF modified electrode at various scan rates. Scan rate (mV•s^{-1}), 10, 20, 40, 60, 80 and 100. Supporting electrolyte, potassium hydrogen phthalate buffer solution (pH 5.0) containing 0.1 mol•L^{-1} KCl. Inset shows the plot of I_{pa} vs. $v^{1/2}$.

relationship can be established between the oxidation peak currents and the square root of scan rates (inset). This indicates that the reaction may be controlled by the diffusion of dopamine in solution.

Conclusions

In this article, nanosized cobalt hexacyanoferrate complex was synthesized and characterized by various techniques including UV/Vis, XRD, ED, FT-IR and ICP-AES. All these results indicate that we obtained a face-centered cubic crystallite with a stoichiometric formula $K_{0.2}Co_{1.4}[Fe(CN)_6]\cdot xH_2O$ which consists of two kinds of CoHCF speices, $Co^{II}_{1.5}[Fe^{III}(CN)_6]$ and $KCo^{III}[Fe^{II}(CN)_6]$. In addition, the electrochemical properties of CoHCF nanoparticles were explored by electrodepositing these particles onto a bare GC electrode in 0.1 mol•L^{-1} KCl solution. The voltammetric responses of the modified electrode show the presence of two redox couples and considerable stability in KCl solution. Effects of concentration of supporting electrolyte and counterions were investigated in detail. Further CoHCF films can catalyze the dopamine oxidation in pH 5.0 potassium hydrogen phthalate buffer solution.

References

1 Neff, V. D. *J. Electrochem. Soc.* **1978**, *125*, 886.
2 Pournaghi-Azar, M. H.; Dastangoo, H. *Electrochim. Acta* **2003**, *48*, 1797.
3 Eftekhari, A. *J. Electroanal. Chem.* **2002**, *537*, 59.
4 Zhang, D.; Wang, K.; Sun, D. C.; Xia, X. H.; Chen, H. Y. *Chem. Mater*. **2003**, *15*, 4163.
5 Wang, P.; Yuan, Y.; Jing, X. Y.; Zhu, G. Y. *Talanta* **2001**, *53*, 863.
6 Chen, S. M.; Hseuh, S. H. *J. Electrochem. Soc.* **2003**, *150*, D175.
7 Itaya, K.; Ataka, T.; Toshima, S. *J. Am. Chem. Soc.* **1982**, *104*, 4767.
8 Pyrasch, M.; Toutianoush, A.; Jin, W. Q.; Schnepf, J.; Tieke, B. *Chem. Mater.* **2003**, *15*, 245.
9 Mortimer, R. J. *J. Electrochem. Soc.* **1991**, *138*, 633.
10 Siperko, L. M.; Kuwana, T. *J. Electrochem. Soc.* **1983**, *130*, 396.
11 Kahrlet, H.; KomorskyLovric, S.; Hermes, M.; Scholz, F. *Fresenius J. Anal. Chem.* **1996**, *356*, 204.
12 Neff, V. D. *J. Electrochem. Soc.* **1985**, *132*, 1382.
13 Kaneko, M.; Okada, T. *J. Electroanal. Chem.* **1988**, *255*, 45.
14 Kalwellis-Mohn, S.; Grabner, E. W. *Electrochim. Acta* **1989**, *34*, 1265.
15 Sato, O.; Einaga, Y.; Fujishima, A.; Hashimoto, K. *Science* **1996**, *272*, 704.
16 Sato, O.; Iyoda, T.; Fujishima, A.; Hashimoto, K. *Inorg. Chem.* **1999**, *38*, 4405.
17 Dujardin, E.; Ferlay, S.; Phan, X.; Desplanches, C.; Cartier dit Moulin, C.; Sainctavit, P.; Baudelet, F.; Dartyge, E.; Veillet, P.; Verdaguer, M. *J. Am. Chem. Soc.* **1998**, *120*, 11374.
18 Escax, V.; Bleuzen, A.; Itie, J. P.; Munsch, P.; Varret, F.; Verdaguer, M. *J. Phys. Chem. B* **2003**, *107*, 4763.
19 Moore, J. G.; Lochner, E. J.; Ramsey, C.; Dalal, N. S.; Stiegman, A. E. *Angew. Chem., Int. Ed.* **2003**, *42*, 2741.
20 Vaucher, S.; Li, M.; Mann, S. *Angew. Chem., Int. Ed.* **2000**, *39*, 1793.
21 Vaucher, S.; Fielden, J.; Li, M.; Dujardin, E.; Mann, S. *Nano Lett.* **2002**, *2*, 225.
22 Zhou, P.; Xue, D.; Luo, H.; Chen, X. *Nano Lett.* **2002**, *2*, 845.
23 Liu, S. Q.; Xu, J. J.; Chen, H. Y. *Electrochem. Commun.* **2002**, *4*, 421.
24 Jiang, M.; Zhou, X.; Zhao, Z. *Ber. Bunsen-Ges. Phys. Chem.* **1991**, *95*, 720.
25 Joseph, J.; Gomathi, H.; Rao, G. P. *J. Electroanal. Chem.* **1991**, *304*, 263.
26 Cai, C. X.; Xue, K. H.; Xu, S. M. *J. Electroanal. Chem.* **2000**, *486*, 111.
27 Chen, S. M. *Electrochim. Acta* **1998**, *43*, 3359.
28 Kulesza, P. J.; Malik, M. A.; Berrettoni, M.; Giorgetti, M.; Zamponi, S.; Schmidt, R.; Marassi, R. *J. Phys. Chem. B* **1998**, *102*, 1870.
29 Lezna, R. O.; Romagnoli, R.; de Tacconi, N. R.; Rajeshwar, K. *J. Phys. Chem. B* **2002**, *106*, 3612.
30 Kulesza, P. J.; Malik, M. A.; Zamponi, S.; Berrettoni, M.; Marassi, R. *J. Electroanal. Chem.* **1995**, *397*, 287.
31 Kulesza, P. J.; Malik, M. A.; Miecznikowski, K.; Wolkiewicz, A.; Zamponi, S.; Berrettoni, M.; Marassi, R. *J. Electroanal. Chem.* **1996**, *143*, L10.
32 Shankaran, D. R.; Narayanan, S. S. *Bull. Chem. Soc. Jpn.* **2002**, *75*, 501.
33 Xu, F.; Gao, M. N.; Wang, L.; Zhou, T. S.; Jin, J. Y. *Talanta* **2002**, *58*, 427.
34 Chen, S. M.; Peng, K. T. *J. Electroanal. Chem.* **2003**, *547*, 179.
35 Xun, Z. Y.; Cai, C. X.; Xing, W.; Lu, T. H. *J. Electroanal. Chem.* **2003**, *545*, 19.
36 Buser, H. J.; Schwarzenbach, D.; Petter, W.; Ludi, A. *Inorg. Chem.* **1977**, *16*, 2704.
37 Zhu, J. J.; Koltypin, Y.; Gedanken, A. *Chem. Mater.* **2000**, *12*, 73.
38 Wilde, R. E.; Ghosh, S. N.; Marshall, B. J. *Inorg. Chem.* **1970**, *9*, 2522.
39 Soto, M. B.; Scholz, F. *J. Electroanal. Chem.* **2002**, *521*, 183.

(E0405243 CHENG, B.)